Revista Mexicana de Astronomía y Astrofísica, **35**, 97–108 (1999)

VLA CONTINUUM OBSERVATIONS OF SUSPECTED MASSIVE HOT CORES

P. Carral[1], S. Kurtz[2], L. F. Rodríguez[2], J. Martí[3], S. Lizano[2], and M. Osorio[2]

Received 1999 March 3; accepted 1999 March 16

RESUMEN

Presentamos observaciones de continuo, hechas con el VLA, hacia 12 fuentes *IRAS* luminosas sin detección previa en el continuo o con continuo relativamente débil. Dadas estas características, las fuentes observadas podrían ser núcleos masivos calientes, conteniendo estrellas OB en las etapas tempranas de su formación. Todas las fuentes fueron observadas a 3.6 cm y cinco de ellas fueron observadas también a 7 mm. Con una excepción (IRAS 20216+4107), todas las fuentes se detectaron a 3.6 cm. Cinco de estas detecciones se reportan aquí por vez primera. La emisión de continuo centimétrica es consistente con la esperada de la fotoionización producida por los miembros más masivos de cúmulos estelares con la luminosidad observada. Sin embargo, existen otras explicaciones posibles (e.g., chorros térmicos) para la relativa debilidad del continuo observado. No se detectó a 7 mm ninguna de las fuentes observadas.

ABSTRACT

We present VLA continuum observations of 12 luminous *IRAS* sources with no previously detected or relatively weak centimeter continuum emission. Given these characteristics, the observed sources could be massive hot cores, containing OB stars in the early stages of formation. All the sources were observed at 3.6 cm and five of them were also observed at 7 mm. With one exception (IRAS 20216+4107), all sources were detected at 3.6 cm. Five of these detections are reported here for the first time. The centimeter continuum emission is consistent with that expected from photoionization by the more massive members of stellar clusters with the observed luminosities. However, other explanations (e.g., thermal jets) are possible for the relatively weak continuum emission observed. No 7 mm emission was detected in the five sources observed.

Key words: **H II REGIONS — RADIO SOURCES: IDENTIFICATIONS — STARS: FORMATION — STARS: MASSIVE**

1. INTRODUCTION

The majority of young stellar objects are associated with detectable free-free centimeter continuum emission (Anglada 1995; 1996). In young low-mass stars the weak but detectable continuum is many orders of magnitude larger than that expected from photoionization. In these sources, the ionization has been attributed to shocks (Curiel, Cantó, & Rodríguez 1987) or heating from ambipolar difusion (Safier 1993), although detailed models have not been worked out.

In contrast, in a number of high luminosity sources ($L > 10^3\ L_\odot$) the thermal radio emission is weaker than expected and in some cases even remains undetected with respect to the expected values for main sequence stars of such luminosity. The apparent lack of observed ionization has been discussed by several groups (e.g., Wood & Churchwell 1989a; Garay et al.

[1] Departamento de Astronomía, Universidad de Guanajuato, México.
[2] Instituto de Astronomía, Universidad Nacional Autónoma de México.
[3] Depto. de Física Aplicada, Escuela Politécnica Superior, Universidad de Jaén, Spain.

TABLE 1

OBSERVED *IRAS* SOURCES

IRAS Source	α (1950) (h m s)	δ (° ′ ″)	$S_{12\mu m}$ (Jy)	$S_{25\mu m}$ (Jy)	$S_{60\mu m}$ (Jy)	$S_{100\mu m}$ (Jy)	Distance (kpc)	L_{IRAS} (10^4 $L_\odot$)	Spectral Type[a]	Dist. Notes
02575+6017	02 57 35.6	+60 17 22	19.9	211.8	767.9	1083	2.2	1.2	B0.5	1
05274+3345	05 27 27.6	+33 45 37	6.9	69.4	449.3	905.7	1.7	0.4	B1	2
05553+1631	05 55 20.3	+16 31 46	$\leq$ 1.3	63.1	420.7	527.5	2.0	0.4	B1	3
18151−1208	18 15 09.0	−12 08 34	19.0	98.6	890.6	1891	3.1	2.6	B0	2,4
18566+0408	18 56 40.8	+04 08 03	14.4	85.3	647.9	1031	6.8	8.4	O7.5	2,5
19410+2336	19 41 04.2	+23 36 54	14.4	108.8	982.5	1631	2.4	1.5	B0.5	2,6
							6.1	10.0	O7	...
20051+3435	20 05 09.4	+34 35 51	4.6	44.5	316.4	506.3	2.6	0.6	B1	2,5
20081+2720	20 08 07.0	+27 20 11	5.8	63.0	845.0	1317	0.9	0.2	B2	6,8
			...	...	...	...	6.0	7.7	O7.5	...
20126+4104	20 12 41.0	+41 04 20	$\leq$ 2.5	108.9	1382	1947	1.7	1.0	B0.5	7
20216+4107	20 21 37.6	+41 07 56	7.4	45.3	295.2	717.9	3.6	1.3	B0.5	2
20343+4129	20 34 19.5	+41 29 33	22.0	151.8	690.9	1035	1.5	0.5	B1	8
21407+5441	21 40 43.7	+54 41 22	5.2	26.5	245.8	$\leq$ 1270	8.5	8.4	O7.5	9

[a] Spectral types are based on the ZAMS luminosities given by Thompson (1984). Distance Notes: (1) Deharveng et al. (1997); (2) Kinematic distance based on the CS velocities of Bronfman et al. (1996) and the rotation curve of Wouterloot et al. (1990); (3) Shepherd & Churchwell (1996); (4) Near distance; at far distance of 13.1 kpc the source would be 400 pc above the galactic plane; (5) Forbidden velocity, distance given is to the tangent point; (6) We are unable to resolve the distance ambiguity; both distances (and luminosities) are reported; (7) Wilking et al. (1989); (8) Miralles et al. (1994). (9) Based on CO line velocity (Kurtz, personal communication) and the rotation curve of Wouterloot et al. (1990).

1993; Kurtz, Churchwell, & Wood 1994; Miralles, Rodríguez, & Scalise 1994) who have suggested several possible explanations: (1) the dust in the H II region is competing with the gas for ionizing photons; (2) the ionization is provided by a cluster of lower mass stars and not by a single high mass star; (3) the ionizing star(s) have not reached the main sequence and have lower temperature(s) than those on the main sequence; (4) part of the free-free emission is spatially extended ($> 1'$) and is missed by radio interferometers with insufficient short spacings; and (5) the H II region is very compact and thus optically thick. In the most compact sources another possible explanation could be a partially optically thick stellar wind or jet. In addition, Walmsley (1995) noted that a massive star embedded in a hot molecular core (HMC), if undergoing intense accretion, might lack a detectable H II region because the accretion quenches its development (see also Yorke 1984). This latter possibility is an intriguing one, since HMCs might be the sites of massive star formation (see the review of Kurtz et al. 1999, and references therein).

In an effort to detect and understand the nature of the radio continuum emission at centimeter wavelengths in young, luminous infrared objects, we report here a Very Large Array 3.6 cm study of twelve regions with *IRAS* luminosities $\geq 2 \times 10^3$ $L_\odot$. Five of the sources were also observed at 7 mm; these sources were selected because at that time they had been observed but not detected at centimeter wavelenghts and because they had a nearby phase calibrator appropriate for the 7 mm observations. It was expected that the 7 mm observations could reveal the presence of emission from heated dust or from an extremely optically thick H II region. Our observations were made with the C and D configurations of the VLA, that have short spacings and will not resolve out extended structures.

To select our sources, we examined the VLA surveys of Wood & Churchwell (1989a), McCutcheon et al. (1991), Kurtz et al. (1994), Miralles et al. (1994), and Kurtz & Churchwell (1999) for bright *IRAS* sources, meeting the Wood & Churchwell (1989b) color criteria for UC H II regions and which were extremely weak or had no detection in these centimeter continuum snapshot surveys.

2. OBSERVATIONS AND DATA REDUCTION

The 12 sources observed with the VLA of the NRAO[4] are listed in Table 1, where we provide the flux densities in the four *IRAS* bands, a distance

[4] The National Radio Astronomy Observatory is a facility of the National Science Foundation operated under cooperative agreement by Associated Universities, Inc.

TABLE 2

SUMMARY OF OBSERVATIONS

IRAS	Pointing Center[a]		Array	Band	Observ.	Phase Calibrator	
Source	R.A.	Dec.	Config.	(cm)	Date	Source	S_ν (Jy)
02575+6017	B02 57 35.6	+60 17 22	D	3.6	11 Jan 1994	0224+671	1.71
05274+3345	B05 27 27.6	+33 45 37	D	3.6	20 Jan 1994	0552+398	6.20
05553+1631	B05 55 20.3	+16 31 46	D	3.6	20 Jan 1994	0528+134	3.75
18151−1208	J18 17 57.1	−12 07 22	CS	3.6	4 Sep 1997	1822−131	0.10
			CS	0.7	4 Sep 1997	1733−130	5.01
18566+0408	B18 56 40.8	+04 08 03	D	3.6	11 Jan 1994	1801+010	0.87
19410+2336	J19 43 11.5	+23 44 06	CS	3.6	4 Sep 1997	1925+211	0.90
			CS	0.7	4 Sep 1997	1925+211	1.02
20051+3435	J20 07 03.8	+34 44 35	CD[b]	3.6	23 Sep 1997	2007+404	2.40
			CD[b]	0.7	23 Sep 1997	2015+371	2.29
20081+2720	B20 08 07.0	+27 20 11	D	3.6	11 Jan 1994	1932+204	0.60
20126+4104	B20 12 41.0	+41 04 20	D	3.6	11 Jan 1994	2005+403	3.22
20216+4107	J20 23 23.8	+41 17 40	CD[b]	3.6	23 Sep 1997	2015+371	3.11
			CD[b]	0.7	23 Sep 1997	2007+404	0.85
20343+4129	B20 34 19.5	+41 29 33	D	3.6	11 Jan 1994	2005+403	3.22
21407+5441	J21 42 23.7	+54 55 07	CS	3.6	4 Sep 1997	2148+611	0.87
...	...	...	CS	0.7	4 Sep 1997	2038+513	1.83
...	...	...	CD[b]	6.0	23 Sep 1997	2148+611	1.12
...	...	...	DnC	3.6	5 Oct 1997	2148+611	0.86

[a] The letter before the right ascension indicates the coordinate epoch: B for B1950, J for J2000.

[b] Observations were made during array re-configuration; the array was intermediate between CS and DnC. The CS configuration is described in http://www.nrao.edu/newsletter/NRAOnews69.html.

(with references in the footnotes) and the resulting infrared luminosity. The latter value is calculated using the formula of Casoli et al. (1986). In addition, we provide the spectral type assuming that a single star provides the total infrared luminosity (Thompson 1984).

In Table 2 we present a summary of the observations, including the phase array pointing center, array configuration, wavelength, observation date, and phase calibrator. For all observations the array was in a relatively compact configuration: either the most compact D configuration or intermediate between the D and C configurations. In 1997 the use of sub-arrays, the absence of some Q-band antennas, and reconfiguration of the array caused the actual *uv*-coverage to differ from what is normally expected. Nevertheless, for all observations there was relatively good coverage of the inner *uv* plane.

The 7 mm observations, made in September 1997, used the fast switching mode with cycle times of two minutes or less. Inspection of the data indicates that this was adequate for the phase stability on each day, hence null detections are probably not caused by loss of phase information. The typical on-source integration times were about one hour and the angular resolution was $\sim 1''$.

The 1994 observations used B1950 coordinates for the pointing centers, while the 1997 observations used J2000 coordinates. In the latter case, the final maps were precessed to B1950 using the AIPS task REGRD. All data were calibrated and mapped using standard procedures in AIPS.

3. RESULTS

3.1. *Observational Data*

Eleven of the 12 fields showed 3.6 cm emission inside the *IRAS* error ellipse. IRAS 20216+4107 was not detected at a 3σ level of 0.3 mJy. These are the first centimeter continuum detections for five of these sources: 18151−1208, 18566+0408, 19410+2336, 20051+3435, and 20126+4104. Only the radio sources associated with IRAS 20051+3435, IRAS 20081+2720, and IRAS 21407+5441 show integrated flux densities in clear excess of the peak flux densities, indicating an extended nature. No 7 mm continuum emission was detected in any of the five fields we observed (see Table 3). The 3σ detection limit at 7 mm was about 1.5 mJy in all cases.

In Table 3 we give the equatorial and galactic coordinates of each radio source, the integrated flux density, and the angular size. Also listed are the synthesized beam and the map *rms* noise. Contour plots of each field are given in Figure 1.

TABLE 3

OBSERVED SOURCE PARAMETERS AT 3.6 CM

IRAS Field	Source Peak Position α (1950) (h m s)	δ (° ′ ″)	Galactic Coordinates	Flux[a] Density (mJy)	Angular Size[b] (arc sec)	Synthesized Beam (arc sec)	Map *rms* (mJy/b)
02575+6017	02 57 37.45	+60 17 24.4	138.300+1.558	4.5	~ 3.3	10.3 × 7.1	0.05
	02 57 34.52	+60 17 24.0	138.295+1.555	0.6	< 7	10.3 × 7.1	0.05
05274+3345	05 27 29.92	+33 45 40.0	174.201−0.070	1.2	< 5	8.2 × 6.8	0.06
...	05 27 27.92	+33 45 37.0	174.198−0.076	0.3	< 5	8.2 × 6.8	0.06
05553+1631	05 55 19.97	+16 31 44.6	192.161−3.816	1.8	< 4	9.4 × 6.9	0.06
18151−1208[c]	18 15 10.0	−12 08 37.9	18.341+1.768	0.5	< 3	3.1 × 2.6	0.07
18566+0408	18 56 40.93	+04 08 03.0	37.553+0.200	0.7	< 6	8.9 × 7.6	0.10
19410+2336[c]	19 41 03.85	+23 36 51.2	59.782+0.064	0.7	< 2	3.1 × 2.5	0.04
...	19 41 03.48	+23 36 48.4	59.781+0.065	0.3[d]	< 3	3.1 × 2.5	0.04
20051+3435[c]	20 05 10.05	+34 35 56.9	71.894+1.311	0.8	~ 10	7.4 × 6.7	0.08
20081+2720	20 08 06.70	+27 20 14.0	66.153−3.183	7.6	~ 26	9.4 × 7.4	0.07
20126+4104	20 12 40.91	+41 04 20.0	78.121+3.632	0.5	< 5	8.7 × 7.4	0.06
20216+4107[c]	...	...	...	< 0.3[e]	...	3.3 × 2.4	0.09
20343+4129	20 34 19.60	+41 29 24.8	80.826+0.566	1.3	< 5	8.9 × 6.7	0.11
21407+5441[c]	21 40 43.60	+54 41 18.2	97.953+1.489	> 660[f]	~ 60	8.5 × 5.8	0.14

[a] The estimated uncertainty in the flux densities is typically $\sim 20\%$.

[b] Deconvolved angular size or upper limit to the angular size.

[c] Source was observed at 7 mm; it was not detected to a 3σ limit of 1.5 mJy beam^{-1}.

[d] The source G59.774+0.047 is detected 1′ SE of the *IRAS* position, at $\alpha(1950) = 19^h\ 41^m\ 06.69^s$, $\delta(1950) = +23°\ 35'\ 53.0''$. Its flux density is 0.6 mJy and its size is $< 2'$.

[e] Emission is present at the 3σ level (0.3 mJy beam^{-1}) but we consider this a null detection at the *IRAS* position. The source G79.092+2.281 is detected 2′ SW of the *IRAS* position at $\alpha(1950) = 20^h\ 21^m\ 30.38^s$, $\delta(1950) = +41°\ 06'\ 22.2''$. Its flux density is 6.0 mJy, obtained with a primary beam correction factor of 1.55.

[f] In our 6 cm map, G98.035+1.446 is detected $\sim 5'$ to the east, at $\alpha(1950) = 21^h\ 41^m\ 21.22^s$, $\delta(1950) = 54°\ 42'\ 31.9''$. It is coincident with the *IRAS* source 21413+5442, and has a 6 cm flux density > 130 mJy. We caution that this 3.4 mm flux density is quite uncertain, because the source is outside the primary beam. Although extended structure is clearly present in the field (cf. NVSS map, Condon et al. 1998), the source we detect appears to be compact. This source is weakly detected at 3.6 cm. Two nonthermal sources are detected to the southwest of the main H II region, at $\alpha(1950) = 21^h\ 40^m\ 37.49^s$, $\delta(1950) = 54°\ 40'\ 49.2''$ (south) and $\alpha(1950) = 21^h\ 40^m\ 36.91^s$, $\delta(1950) = 54°\ 41'\ 13.2''$ (north). The southern source has flux densities of 5.3 ± 0.5 mJy and 2.6 ± 0.5 mJy at 6 and 3.6 cm, respectively. The northern source has flux densities of 6.1 ± 0.6 mJy and 1.4 ± 1.0 mJy at 6 and 3.6 cm, respectively.

3.2. *Individual Sources*

3.2.1. IRAS 02575+6017

This source is also known as AFGL 4029. In a recent review of this region, Deharveng et al. (1997) found that the *IRAS* emission is not associated with a single object but with a cluster of massive stars. The source is located in the molecular cloud IC 1848A (Loren & Wootten 1978); to the west is a bright rim associated with the H II region S 159. We detect this rim as an arc of emission at 3.6 cm, but it is too large to be properly imaged by our observations. We detect two compact radio sources roughly coincident with the *IRAS* uncertainty ellipse. These were independently detected by Kurtz et al. (1994) at higher resolution. The western radio source, with a flux density of 0.6 mJy, probably drives the CO outflow (Snell et al. 1988) and optical jet (Ray et al. 1990), since it is located at the centroid of the outflow activity and at the origin of the jet. It coincides in position with a deeply embedded ($A_v > 25$ mag), high luminosity ($> 10^4\ L_\odot$) infrared object (IRS 1) and the associated nebulosity exhibits many characteristics of a pre-main sequence object (Deharveng et al. al. 1997). Based on optical spectra, Deharveng et al. show that the optical nebulosity associated with the eastern compact radio component is an H II region excited by a B1V star. This is consistent with the 4.5 mJy flux density that we detect, which could be produced by the ionizing photons of a B1 star.

3.2.2. IRAS 05274+3345

Hunter et al. (1995) report a detailed radio and NIR study of this region, also known as AFGL 5142. They find a cluster of IR sources, many of which have strong IR excess, typical of YSOs still surrounded by their parent molecular gas and dust. The brighter source we detect is to the east of the *IRAS* position ellipse (see Figure 1 and Table 3), and was also detected by Hunter et al. (1995) and Torrelles et al. (1992) at 3.6 cm and by McCutcheon et al. (1991) at 6 cm. It lies at the center of a cluster of H_2O masers and is coincident with a NIR source, IRS 1, and a dense molecular core (Verdes-Montenegro et al. 1989; Torrelles et al. 1992; Estalella et al. 1993; Eiroa et al. 1994; Hunter et al. 1995). Hunter et al. identify two molecular outflows in the region and suggest that IRS 1 powers one of them. They argue that IRS 1 is a YSO in an early evolutionary phase and that it dominates the *IRAS* emission. From our 3.6 cm flux density of 1.2 mJy and McCutcheon et al.'s 6 cm measurement of 0.49 mJy we obtain a spectral index of 1.7, suggestive of an optically thick H II region.

Within the *IRAS* ellipse we have a marginal (4σ) detection at 3.6 cm with a peak flux density of 0.3 mJy (see Figure 1). This position is about 3″ south of another NIR source (IRS 2) detected by Hunter et al. The difference in position can probably be accounted for by the errors (about one arc second in each case). Hunter et al. suggest that IRS 2 may power the extended (SE-NW) CO outflow (Snell et al. 1988) and probably dominates the mid-infrared flux from the region. They suggest that this object is a YSO in an advanced phase of evolution. High resolution CO observations and high sensitivity, multi-frequency, radio continuum observations would likely prove useful to understand the nature of these objects.

3.2.3. IRAS 05553+1631

This region has been reported in the literature as AFGL 5173 and G192.16−3.81. It has an associated reflection nebula, an outflow (Snell, Dickman, & Huang 1990; Shepherd & Churchwell 1996), and water maser emission (Codella, Felli, & Natale 1996). The nebulosity was imaged by Hodapp (1994) in the K′ bands who reports a bipolar morphology. The local molecular gas properties have been derived by Carpenter et al. (1993), Carpenter, Snell, & Schloerb 1995). McCutcheon et al. (1991) detected an H II region associated with the *IRAS* source and measured a flux density of 1.4 ± 0.1 mJy at 6 cm. At 0.″3 spatial resolution, the 6-cm map of Hughes & MacLeod (1993) shows internal structure. Shepherd & Kurtz (1999) observed the region at 3.6 cm and 7 mm in the continuum and also in the water maser line; they report the detection of a 1000 AU circumstellar disk. From our 3.6 cm measurement of 1.8 mJy and McCutcheon et al.'s 6 cm observation, we estimate a spectral index of $\alpha = 0.5 \pm 0.3$, consistent with the source having a biconical jet dominating the radio emission (Reynolds 1986).

3.2.4. IRAS 18151−1208

IRAS 18151−1208 lies in the direction of the extended H II region S 54 which was mapped at 21 cm by Felli & Churchwell (1972). Water masers and ammonia (1,1) and (2,2) emission have been detected toward the *IRAS* position (Codella et al. 1996; Molinari et al. 1996). McCutcheon et al. (1995) mapped the emission at 1100, 800, and 450 μm. Extrapolating McCutcheon et al.'s fit to longer wavelengths, we predict a 7 mm flux density of about 2 mJy. This is slightly higher than the 1.5 mJy detection limit of our observations, where no evidence of 7 mm emission was seen.

McCutcheon et al. (1991) failed to detect 6 cm emission toward this source at an *rms* level of 0.3 mJy. In our 3.6 cm map we find evidence for extended structure probably associated with S 54. Removing the shorter baselines from the *uv* data, the resulting 3.6 cm map shows a compact source with a flux density of 0.5 mJy which falls within the *IRAS* uncertainty ellipse. The centroid of the 800 μm emission mapped by McCutcheon et al. (1995) is coincident with the 3.6 cm radio source, suggesting that they are associated. From McCutcheon et al.'s upper limit and our 3.6 cm measurement, we obtain a spectral index $\alpha \gtrsim 1.0$.

3.2.5. IRAS 18566+0408

Miralles et al. (1994) did not detect 6 cm or 2 cm emission toward this source, at 5σ detection levels of 0.5 mJy and 0.8 mJy, respectively. We detect a 0.7 mJy source coincident with the *IRAS* position. Miralles et al. report water maser and ammonia (1,1) and (2,2) emission (see also Molinari et al. 1996). Scalise, Rodríguez, & Mendoza-Torres (1989) and Palla et al. (1991) report IRAS 18566+0408 as a source without water maser emission. However, this is not unusual, given the variability of water maser emission. Evidence of dense gas in the region comes from the detection of the CS(2–1) line by Bronfman, Nyman, & May (1996).

3.2.6. IRAS 19410+2336

Observations toward this source indicate the presence of warm, dense gas, as well as H_2O, OH, and CH_3OH maser emission (Lada et al. 1981; Bronfman et al. 1996; Braz & Sivagnanam 1987; Menten 1991; Caswell et al. 1995a,b). The water and methanol maser positions are shown by crosses in the 3.6 cm continuum map of Figure 1. The methanol masers reported by Caswell et al. (1995a,b) are essentially

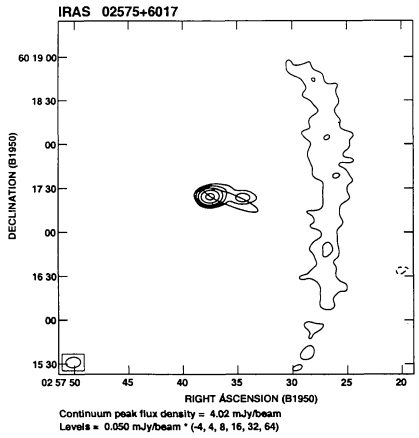

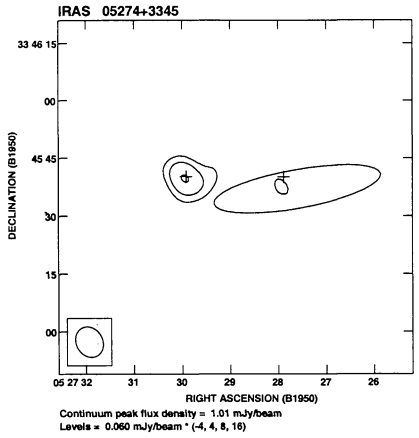

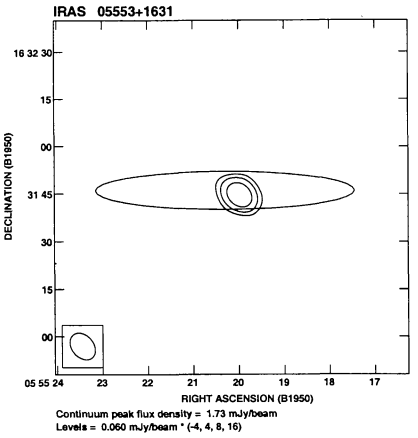

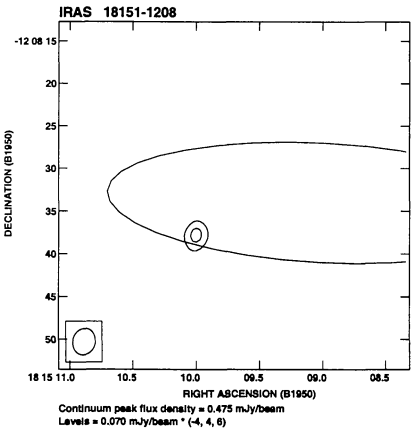

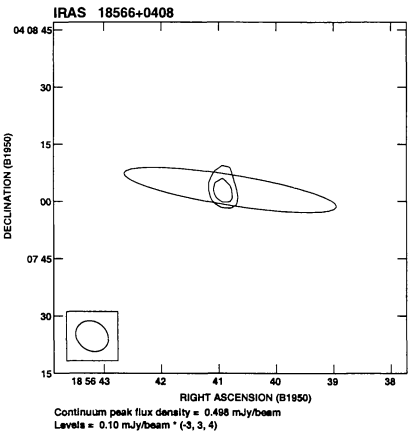

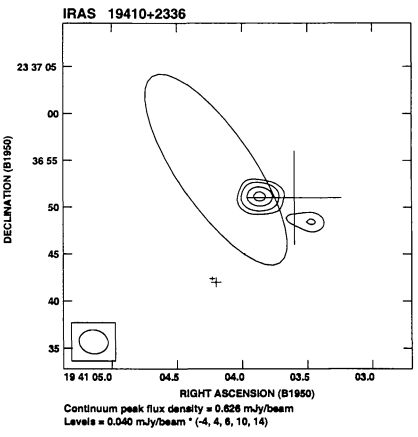

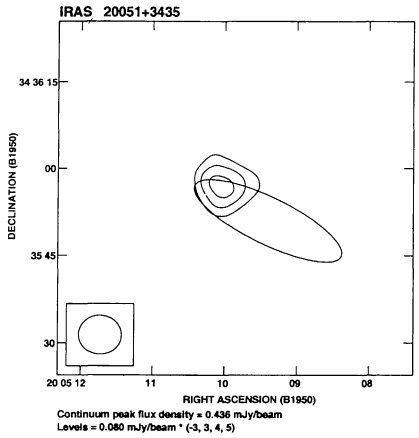

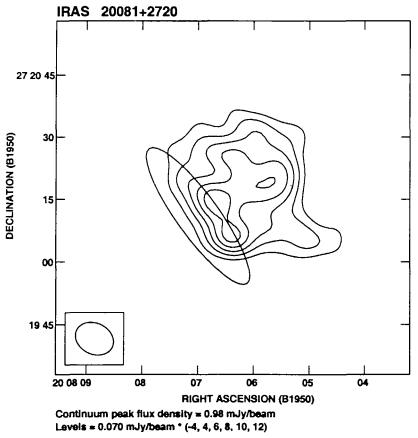

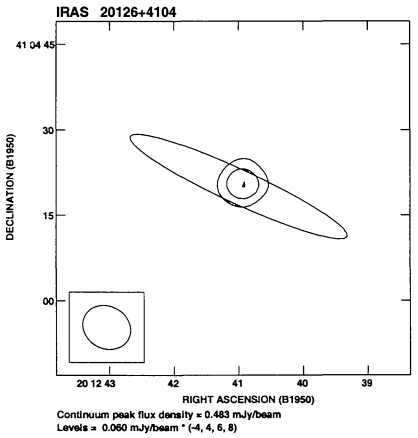

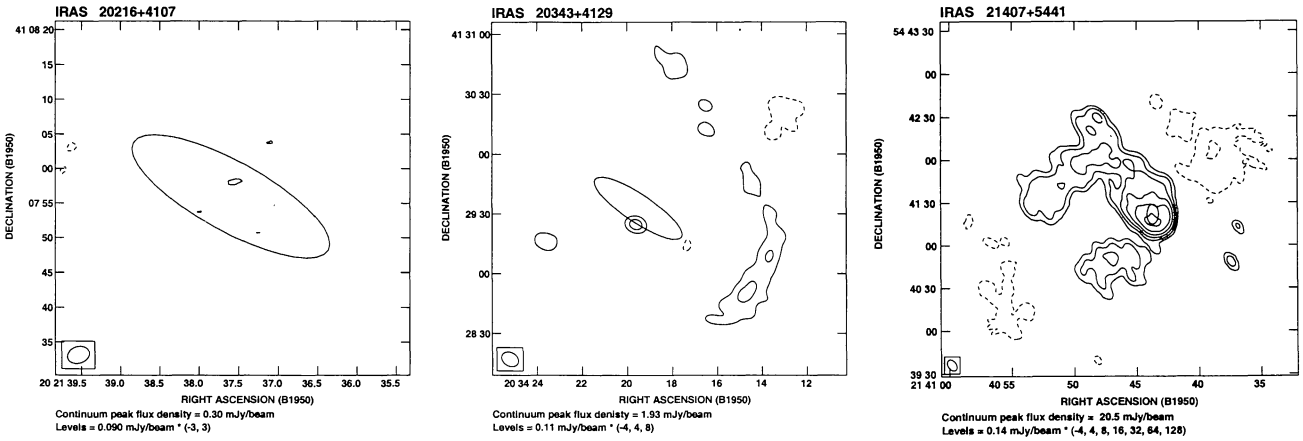

Fig. 1. The twelve *IRAS* fields we observed are shown in 3.6 cm radio continuum contour plots. The *IRAS* name is indicated at the upper left of each box and the contour levels (in multiples of the map *rms*) are shown immediately below each box. The synthesized beam size is indicated in the lower left corner. The ellipse shown in each field is the *IRAS* 1σ positional uncertainty. For IRAS 05274+3345 the small crosses indicate the positions of IRS 1 and IRS 2, taken from Hunter et al. (1995). For IRAS 19410+2336 the crosses indicate maser positions, with the size of each cross indicating the positional uncertainty. The largest cross (essentially coincident with the 3.6 cm continuum components), indicates the 6.6 and 12 GHz CH_3OH maser detections of Caswell et al. (1995a,b). The smallest cross is an H_2O maser reported by Lada et al. (1981); the slightly larger cross located to the southwest of the H_2O maser is a 6.6 GHz CH_3OH maser reported by Menten (1991).

coincident with radio continuum components that we detect. The water maser (Lada et al. 1981) and another methanol maser (Menten 1991) are found about 10″ to the southeast of the radio continuum components, at a location where we do not detect centimeter continuum emission. This may indicate that another massive star formation site is present in the field, immediately south of the *IRAS* position. Variability of methanol masers has been reported (Caswell et al. 1995a,b), so it is not surprising that methanol masers were found in distinct locations by different workers.

CO observations by Kurtz (personal communication) show evidence of high velocity molecular gas in the region. Kurtz et al. (1994) report a null detection toward this source, although they did detect very weak (4σ) emission at 3.6 cm, coincident with the *IRAS* position. We detect three unresolved sources, one with a flux density of 0.7 mJy, coincident with Kurtz et al.'s marginal detection and coincident with the *IRAS* position. This source is located about 9″ north of the H_2O and OH masers, and coincides within the errors with the CH_3OH maser emission. Hughes & MacLeod (1994) provide an upper limit of 0.7 mJy for this source at 6 cm, which implies a positive spectral index. The second 3.6 cm source, with a flux density of 0.3 mJy, is located slightly outside of the *IRAS* uncertainty ellipse, about 10″ south-west of the *IRAS* position. A third 3.6 cm source, with a flux density of 0.6 mJy, is located about 1′ south-east of the *IRAS* position (see the footnotes of Table 3) and is probably unrelated.

3.2.7. IRAS 20051+3435

This source was observed by McCutcheon et al. (1991) who did not detect 6 cm emission with the VLA at a 0.3 mJy limit. They observed the CO(1–0) line and found a broad ($\Delta V_{200mK} = 17.3$ km s^{-1}), complex profile. Evidence of dense gas is indicated by the detection of CS(2–1) emission by Bronfman et al. (1996). Our observations show a source located at the edge of the *IRAS* uncertainty ellipse. The measured flux density and size are 0.8 mJy and $\sim 10''$, respectively. Using McCutcheon et al.'s upper limit at 6 cm and our 3.6 cm flux density, we obtain a spectral index of $\alpha > 1.9$. Such a spectral index suggests an optically thick H II region in the spectral range observed. Since the source was not detected at 7 mm at a level of less than 1.5 mJy, the turnover frequency of the free-free emission is probably around 3.6 cm, implying an emission measure of $\sim 2 \times 10^8$ cm^{-6} pc.

3.2.8. IRAS 20081+2720

This object was observed at 6 cm with the VLA in its C configuration by McCutcheon et al. (1991). They measured a flux density of 6.6 mJy and an angular size of 30″. Miralles et al. (1994) did not detect it with the VLA at 6 cm (C configuration) or 2 cm (D configuration), possible because of lack of sensitivity and the fact that the source is quite extended and relatively faint. Evidence for dense gas in the region comes from ammonia (1,1) and (2,2) detections by Miralles et al. (1994) and a CS(2–1) detection

by Bronfman et al. (1996). Our 3.6 cm map shows a 7.6 mJy relatively extended ($\sim 26''$) source, with the peak radio emission coincident with the *IRAS* ellipse. The nearly equal flux densities at 6 and 3.6 cm suggest an optically thin source.

3.2.9. IRAS 20126+4104

This object is located in the Cygnus region. Our 3.6 cm map reveals a faint ($S_\nu = 0.5 \pm 0.1$ mJy) unresolved source. A molecular outflow is reported by Wilking, Blackwell, & Mundy (1990). Tofani et al. (1995) detect a line of water masers coincident with the *IRAS* position, but did not detect 3.6 cm continuum in their snapshot observations. Cesaroni et al. (1997) present a detailed study of the region using radio molecular lines and continuum observations in addition to NIR images. Their interpretation suggests a B2.5–B0.5 (proto)star at the center of a dense, rotating disk; along the disk axis the matter is swept away by a molecular outflow. Our 3.6 cm position coincides, within the uncertainty, with the compact core that Cesaroni et al. (1997) identify with a rotating disk. The disk interpretation of Cesaroni et al. is supported by VLA observations of Zhang, Hunter, & Sridharan (1998), who report the kinematics of ammonia emission. Recent high resolution radio observations showed that the source splits into two elongated objects that may indicate thermal jets (Hofner et al. 1999).

3.2.10. IRAS 20216+4107

This source lies in the Cygnus region. The observed CO profiles at this position have high-velocity wings suggesting the presence of an outflow (Wilking et al. 1989; McCutcheon et al. 1991). Dense gas in the region is traced by CS(2–1) emission (Bronfman et al. 1996). McCutcheon et al. (1995) mapped the 1100 μm and 800 μm dust emission and fit the spectrum from 12 μm to 1100 μm using two dust components. One component is hot ($T_{dust} = 123$ K) and compact, while the other is colder ($T_{dust} = 28$ K) and more extended (0.44 pc at a distance of 3.3 kpc). Extrapolating the spectrum of the cold component to 7 mm we anticipate a flux density of about 0.8 mJy, which is below our detection limit. No 3.6 cm emission was detected toward the *IRAS* position to a 3σ level of 0.3 mJy. We do detect a 6 mJy source in the field (see Table 3, footnotes) but $2'$ distant from the *IRAS* position and probably unrelated. This is the only source in our survey where we failed to detect a 3.6 cm source inside the *IRAS* error ellipse.

3.2.11. IRAS 20343+4129

This source was detected at 6 cm by Miralles et al. (1994) with the VLA in C configuration. They report a flux density of 1.1 ± 0.2 mJy and size of $< 5''$. Our 3.6 cm map shows a compact component with a flux density of 1.1 ± 0.1 mJy and an arc of emission probably associated with an independent ionizing source (see Fig. 1). The compact component has a spectral index consistent with an optically-thin H II region. Extended emission is seen in the NVSS map (Condon et al. 1998). This emission is too large for us to image properly with the present observations and is almost certainly responsible for the arc of emission that we see. The relationship between the compact component that we detect, and the more extended region, is unclear. Several molecular lines have been observed toward this source: ammonia (1,1) and (2,2) by Miralles et al. (1994), CS(2–1) by Bronfman et al. (1996), and HCO^+(1-0) by Richards et al. (1987). All lines have the same V_{LSR} of +11 km s^{-1}.

3.2.12. IRAS 21407+5441

This source was not detected by Kurtz & Churchwell (1999) at 3.6 cm in the VLA B-configuration, whose observations were sensitive to structures $\lesssim 20''$. We detect extended emission at 3.6 and 6 cm, coincident with the *IRAS* position. Extended emission is clearly evident in the 21 cm NVSS map (Condon et al. 1998). The null detection by Kurtz & Churchwell is clearly a consequence of their insensitivity to large structures. Bronfman et al. (1996) do not detect CS(2–1) emission at this position, consistent with the view that CS emission traces the dense gas associated with *ultracompact* H II regions, while the region detected here has clearly developed beyond the ultracompact stage.

In addition, we detect the source G98.035+1.446 some $5'$ to the east, coincident with IRAS 21413+5442. This source, at an assumed distance of 8.5 kpc, has an *IRAS* luminosity of $2.4 \times 10^5\ L_\odot$. This field lies outside both the 6 cm and the 3.6 cm primary beams; in the footnotes of Table 3 we note its position but give only an estimate of its flux density, as the primary beam correction factor is unreliable. In the NVSS 21 cm map, emission extends from the eastern *IRAS* source, 21407+5441 westward, up to and including the source 21413+5442. The two *IRAS* sources are evident as local maxima within the more extended emission. We reproduce the NVSS map of this field, and our 6 cm map, in Figure 2.

Two point sources are detected about $1'$ southwest of the 21407+5441 H II region; both have strongly non-thermal spectra. This behavior, coupled with their distance from the *IRAS* position, suggests that they are unrelated.

4. DISCUSSION

We detected 3.6 cm emission within the *IRAS* positional uncertainty ellipse in eleven of the twelve *IRAS* sources observed. In two of the sources (20081+2730 and 21407+5441) we detected extended emission not seen in previous high angular reso-

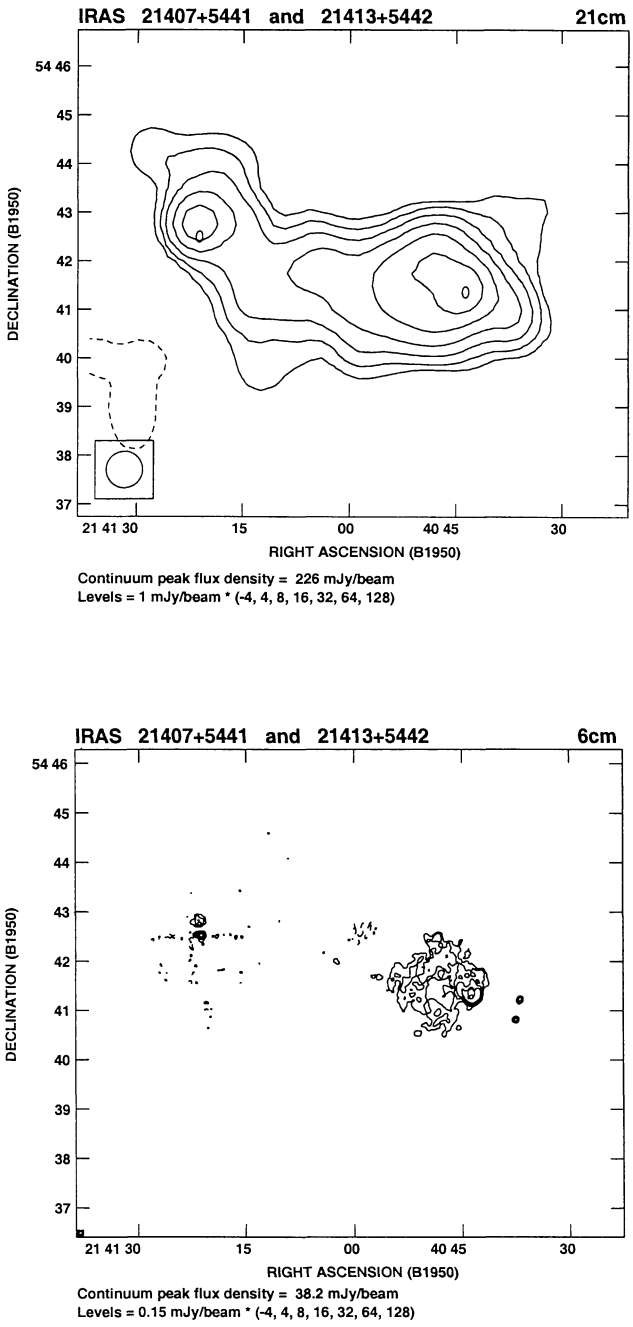

Fig. 2. Large scale structure in IRAS 21407+5441. (*Top*) The NVSS 21 cm image (beamsize $45'' \times 45''$) shows extended structure extending from the position of IRAS 21407+5441 (coincident with the western radio peak) eastward, up to and including IRAS 21413+5442 (coincident with the eastern radio peak). The *IRAS* error ellipses are seen nearly coincident with the two radio peaks. (*Bottom*) Our 6 cm image of the same region (beamsize $4\farcs4 \times 4\farcs1$) is sensitive only to structures $\lesssim 5'$ in size; it is almost certainly missing some flux that can only be sampled with shorter baselines.

lution observations. As recently shown by Kurtz et al. (1999), a potentially significant problem of the UC H II region snapshot surveys is that they were made with relatively extended configurations of the VLA and hence were not sensitive to large-scale structures. The Kurtz & Churchwell (1999) observations of IRAS 21407+5411, for example, were insensitive to structures larger than about $20''$. The H II region we detect is about $2'$ in diameter, far larger than Kurtz & Churchwell could see. We note that this radio source *was* detected and mapped by the NRAO VLA Sky Survey (NVSS). It would be worthwhile to search the NVSS for all observations corresponding to *IRAS* sources with Wood & Churchwell (1989b) colors, especially those which were not detected in high-resolution VLA surveys.

In Figure 3 we show a plot of ionizing photon rate versus luminosity for all the observed sources, except IRAS 21407+5441 where we do not have a reliable value for the total ionizing photon rate. The lines in the figure correspond to three models: (1) a single ZAMS star, (2) a binary system formed by two identical stars, and (3) a cluster of stars with the IMF of Miller & Scalo (1979) and a low mass cutoff at 0.9 $M_\odot$. We have used the stellar parameters tabulated by Thompson (1984). For sources with a distance ambiguity we connect the two data points by a dashed line. For these calculations we assume that dust does not compete significantly for the ionizing photons and that the free-free emission is optically thin. The error bars for the data points were obtained assuming errors of 10% in the *IRAS* and radio flux densitites and of 25% in the distances. As seen in the figure and as discussed previously in the literature, the hypothesis of a single star cannot account for most of the observations because for a given luminosity, the observed ionizing photon rate is much smaller than expected. However, if one assumes that the luminosity is provided by a stellar cluster, we find that within error, all the data points fall in the band contained between the single star model and the cluster model. From the figure we conclude that our observations can be explained in terms of stellar clusters. However, as we will discuss below, some of these relatively weak radio continuum sources could also be thermal jets. In the case of IRAS 20216+4107, where we have only an upper limit, more sensitive observations are required to determine if this source falls below the line defined by the cluster model. Another factor that is probably contributing to the apparent lack of ionizing photons is that some of the sources appear to be optically thick, as in the case of IRAS 05274+3345, IRAS 18151–1208, and IRAS 20051+3435. In these sources the derived ionizing photon rates is probably a lower limit; however, given that the spectral indices were derived from inhomogeneous data sets and are thus not fully reliable, we will consider the derived

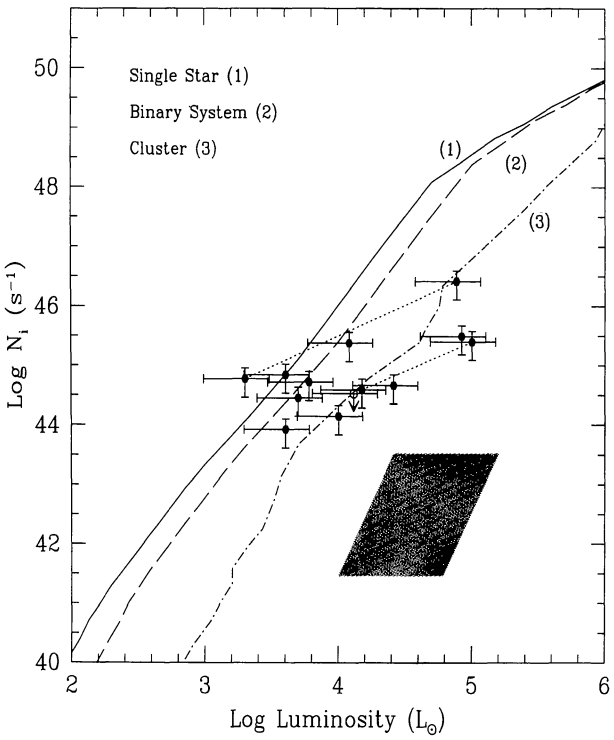

Fig. 3. Ionizing photon rate versus infrared luminosity for the observed sources. Here we plot the infrared luminosity of the observed *IRAS* sources versus the ionizing photon flux calculated from the observed 3.6 cm flux densities under the assumption of optically thin free-free emission with no photons absorbed by dust. The open circle corresponds to IRAS 20216+4107, for which we only have an upper limit to the ionizing flux. We also plot luminosity-ionizing photon rate curves corresponding to the cases of a single early-type star (curve 1, solid line), an equal mass binary system (curve 2, dashed line), and a cluster of stars (curve 3, dot-dashed line). We have used the stellar parameters tabulated by Thompson (1984) in all cases, and for the cluster curve we assumed the IMF of Miller & Scalo (1979) with a low mass cutoff of 0.9 $M_\odot$. Data points connected by dashed lines indicate sources for which we could not resolve the kinematic distance ambiguity. The data for IRAS 21407+5441 are not plotted. The shaded area shows the location of the models of typical CHMCs (Osorio et al. 1999).

ionizing photon rates as estimates of the true values.

An alternative explanation is that we may not be observing photoionized H II regions but instead thermal jets. These thermal jets would produce detectable centimeter continuum emission but with a flux density one or two orders of magnitude below that expected for an optically-thin H II region ionized by a single ZAMS star with the observed luminosity, as is the case for the flux densities observed in the sources discussed here. Then, it is possible that several of the sources detected here are thermal jets, whose presence could be confirmed with high angular resolution continuum observations. Indeed, in both IRAS 05553+1631 (Shepherd & Kurtz 1999) and IRAS 20126+4104 (Hofner et al. 1999) high angular resolution VLA observations strongly suggest that the sources of radio continuum emission are thermal jets (Anglada 1995; 1996), i.e., collimated flows of ionized gas emanating from the young stars. In this case the interpretation of the free-free emission becomes complicated because the nature of the ionization mechanism of jets is unclear. In low mass stars it is believed that shocks play a key role, while in massive stars such as those discussed here, both shock ionization and photoionization could be important.

We also note that, with the possible exception of IRAS 20216+4107 (and IRAS 05274+3345 in the case the far distance is the correct one) none of the sources observed appears likely to be a *collapsing* HMC (CHMC) as modeled by Osorio, Lizano, & D'Alessio (1999). In the CHMC model, Osorio et al. develop the suggestion of Walmsley (1995) and model a single massive star accreting mass at high rates. Its Strömgren radius is therefore, reduced to close to the stellar radius. In this case, the free-free emission from the ionized material is undetectable at centimeter wavelengths and one would expect to find such an object below the "cluster line" drawn in Figure 3. This is not the case for any of our objects, except possibly for IRAS 20216+4107. The shaded area in Figure 3 shows the location of the models of typical CHMCs, interpreting the 3.6 cm dust continuum emission as if it were due to free-free emission from ionized gas. This allows to arbitrarily "assign" an ionizing photon rate to the models, so that they could be placed in Figure 3, although we stress that this is not the actual physical situation predicted by the model. This figure shows that one would assign to the modeled CHMCs a rate of ionizing photons orders of magnitude below that of the objects in the observed sample. In fact, the centimeter continuum emission is so low that it is not feasible to try a detection in this type of cores. Instead, millimetric surveys with high spatial resolution would be a better approach to find them.

Studies of *individually* forming stars and their collapsing envelopes are problematic because of the range of angular resolutions in presently available data. Radio observations can have sufficient resolution to isolate single star formation sites, but mid and far-infrared data are of lower resolution and may include emission from other stars forming in or near the same core. This confusion may be less serious for CHMCs with luminosities $L \geq 10^5 L_\odot$, that would dominate the total luminosity of the region. Unfortunately, very few of these sources are expected, as shown by Osorio et al. (1999). For typical CHMCs,

their models predict very large ratios of 60 μm flux to 25 μm flux, log[60/25] $\geq$ 1.70; the sources studied in this work have log[60/25] $\leq$ 1.13. Flux contamination by nearby cluster members; however, will affect the color estimate if observed with low spatial resolution. Only in spatially separated CHCMs would one expect to measure the predicted log[60/25] ratio. As mentioned before, five sources where observed at 7 mm but no emission was detected. Models for typical CHMCs predict 7 mm flux densities of about $\sim$ 1 mJy. Such fluxes fall slightly below our noise level of $\sim$ 1.5 mJy. The observing time required to detect the cores at 7 mm is presently large, but when the full complement of 7 mm receivers is installed at the VLA a survey program will be feasible.

Finally, it should also be pointed out that the presence of thermal jets in a given source does not necessarily imply that the source is not a CHMC (see Osorio et al. 1999). The large accretion rates expected in these sources ($\dot{M} \simeq 10^{-3}\ M_{\odot}\ \mathrm{yr}^{-1}$) would almost certainly produce an angular momentum problem, that could be disposed of by means of collimated ejection, as in the case of low mass stars. Further research, made with high angular resolution, is necessary to disentangle the possible roles played by stellar clusters, thermal jets, and CHMCs in these regions of massive star formation.

5. SUMMARY

We present sensitive 3.6 cm VLA observations of 12 bright *IRAS* sources suspected of being massive hot cores. In all sources but one, we detect emission inside the *IRAS* error ellipse. We also observed five of these sources at 7 mm, setting upper limits of order 1.5 mJy in all cases. The observations are consistent with ionization from the more massive member(s) of a stellar cluster. However, in some of the sources other phenomena, such as thermal jets, are present. We discuss our observations in the framework of the search for collapsing hot molecular cores and comment on the need for multifrequency, high-angular resolution observations to detect and study them.

We thank G. Anglada, G. Garay, and an anonymous referee for their comments. PC acknowledges the support of CONACyT grant 458100-5-0460PE. SK, LFR, SL, and MO acknowledge partial support from CONACyT, México and DGAPA, UNAM. J.M. acknowledges partial support by DGICYT (PB97-0903) and Junta de Andalucía, Spain.

REFERENCES

Anglada, G. 1995, in Circumstellar Disks, Outflows and Star Formation, ed. S. Lizano & J. M. Torrelles, RevMexAASC, 1, 67

_____. 1996, in ASP Conf. Ser. Vol. 93, Radio Jets in Young Stellar Objects. In Radio Emission from the Stars and the Sun, ed. A. R. Taylor & J. M. Paredes (San Francisco: ASP), 3

Braz, M. A., & Sivagnanam, P. 1987, A&A, 181, 19

Bronfman, L., Nyman, L.-Å., & May, J. 1996, A&AS, 115, 81

Carpenter, J. M., Snell, R. L., Schloerb, F. P., & Skrutskie, M. F. 1993, ApJ, 407, 657

Carpenter, J. M., Snell, R. L., & Schloerb, F. P. 1995, ApJ, 450, 201

Casoli, F., Combes, F., DuPraz, C., Gerin, M., & Boulanger, F. 1986, A&A, 169, 281

Caswell, J. L., Vaile, R. A., Ellingsen, S. P., Whiteoak, J. B., & Norris, R. P. 1995a, MNRAS, 272, 96

Caswell, J. L., Vaile, R. A., Ellingsen, S. P., & Norris, R. P. 1995b, MNRAS, 274, 1126

Cesaroni, R., Felli, M., Testi, L., Walmsley, C. M., & Olmi, L. 1997, A&A, 325, 725

Codella, C., Felli, M., & Natale, V. 1996, A&A, 311, 971

Condon, J. J., Cotton, W. D., Greisen, E. W., Yin, Q. F., Perley, R. A., Taylor, G. B., & Broderick, J. J. 1998, AJ, 115, 1693

Curiel, S., Cantó, J., & Rodríguez, L. F. 1987, RevMexAA, 14, 595

Deharveng, L., Zavagno, A., Cruz-González, I., Salas, L., Caplan, J., & Carrasco, L. 1997, A&A, 317, 459

Eiroa, C., Torrelles, J. M., Miranda, L. F., Anglada, G., & Estalella, R. 1994, A&AS, 108, 73

Estalella, R., Mauersberger, R., Torrelles, J. M., Anglada, G., Gómez, J. F., López, R., & Muders, D. 1993, ApJ, 419, 698

Felli, M., & Churchwell, E. 1972, A&AS, 5, 369

Garay, G., Rodríguez, L. F., Moran, J. M., & Churchwell, E. 1993, ApJ, 418, 368

Hodapp, K-W. 1994, ApJS, 94, 615

Hofner, P., Cesaroni, R., Rodríguez, L. F., & Martí, J. 1999, A&A, in press

Hughes, V. A. & MacLeod, G. C. 1993, AJ, 105 1495

_____. 1994, ApJ, 427, 857

Hunter, T. R., Testi, L., Taylor, G. B., Tofani, G., Felli, M., & Phillips, T. G. 1995, A&A, 302, 249

Kurtz, S., Cesaroni, R., Churchwell, E., Hofner, P., & Walmsley, C. M. 1999, in Protostars & Planets IV, ed. V. Mannings, A. Boss, & S. Russell (Tucson: Univ. of Arizona Press)

Kurtz, S., & Churchwell, E. 1999, in preparation

Kurtz, S., Churchwell, E., & Wood, D .O. S. 1994, ApJS, 91, 659

Kurtz, S., Watson, A., Hofner, P., & Otte, B. 1999, ApJ, 514, in press

Lada, C. J., Blitz, L., Reid, M. J., & Moran, J. M. 1981, ApJ, 243, 769

Loren, R. B., & Wootten, H. A. 1978, ApJ, 225, L81

McCutcheon, W. H., Dewdney, P. E., Purton, C. R., & Sato, T. 1991, AJ, 101, 1435

McCutcheon, W. H., Sato, T., Purton, C. R., Matthews, H. E., & Dewdney, P. E. 1995, AJ, 110, 1762

Menten, K. M. 1991, ApJ, 380, L75

Miller, G. E. & Scalo, J. M. 1979, ApJS, 41, 513

Miralles, M. P., Rodríguez, L. F., & Scalise, E. 1994, ApJS, 92, 173

Molinari, S., Brand, J., Cesaroni, R., & Palla, F. 1996, A&A, 308, 573

Osorio, M., Lizano, S., & D'Alessio, P. 1999, ApJ, submitted

Palla, F., Brand, J., Comoretto, G., Felli, M., & Cesaroni, R. 1991, A&A, 246, 249
Richards, P. J., Little, L. T., Toriseva, M., & Heaton, B. D. 1987, MNRAS, 228, 43
Ray, T. P., Poetzel, R., Solf, J., & Mundt, R. 1990, ApJ, 357, L45
Reynolds, S. P. 1986, ApJ, 304, 713
Safier, P. N. 1993, ApJ, 408, 115
Scalise, E. Jr., Rodríguez, L. F., & Mendoza-Torres, E. 1989, A&A, 221, 105
Shepherd, D. S., & Churchwell, E. 1996, ApJ, 472, 225
Shepherd, D. S., & Kurtz, S. 1999, ApJ, submitted
Snell, R. L., Dickman, R. L., & Huang, Y.-L. 1990, 352, 139
Snell, R. L., Huang, Y.-L., Dickman, R. L., & Claussen, M. J. 1988, ApJ, 325, 853
Thompson, R. I. 1984, ApJ, 283, 165
Tofani, G., Felli, M., Taylor, G. B., & Hunter, T. R., 1995, A&AS, 112, 299
Torrelles, J. M., Gómez, J. F., Anglada, G., Estalella, R., Mauersberger, R., & Eiroa, C. 1992, ApJ, 392, 616
Verdes-Montenegro, L., Torrelles, J. M., Rodríguez, L. F., Anglada, G., López, R., Estalella, R., Cantó, J., & Ho, P. T. P. 1989, ApJ, 346, 193
Walmsley, C. M. 1995, RevMexAASC 1, Circumstellar Disks, Outflows and Star Formation, ed. S. Lizano & J. M. Torrelles (México, D. F.: Inst. Astron., UNAM), 137
Wilking, B. A., Blackwell, J. H., & Mundy, L. G. 1990, AJ, 100, 758
Wilking, B. A., Mundy, L. G., Blackwell, J. H., & Howe, J. E. 1989, ApJ, 345, 257
Wood, D. O. S., & Churchwell, E. 1989a, ApJS, 69, 831
_____. 1989b, ApJ, 340, 265
Wouterloot, J. G. A., Brand, J., Burton, W. B., & Kwee, K. K. 1990, A&A, 230, 21
Yorke, H. 1984, Workshop on Star Formation, ed. R. D. Wolstencroft (Edinburgh: Royal Observatory), 63
Zhang, Q., Hunter, T. R., & Sridharan, T. K. 1998, ApJ, 505, 151

Patricia Carral: Departamento de Astronomía, Universidad de Guanajuato, Apdo. Postal 144, Guanajuato, Guanajuato, 36000 México (patricia@antares.astro.ugto.mx).
Stanley Kurtz, Susana Lizano, Mayra Osorio, and Luis F. Rodríguez: Instituto de Astronomía, UNAM, Unidad Morelia, J. J. Tablada 1006, Morelia, Michoacán, 58090, México (kurtz,lizano,luisfr,mayra@astrosmo.unam.mx.)
Josep Martí: Depto. de Física Aplicada, Escuela Politécnica Superior, Universidad de Jaén, Calle Virgen de la Cabeza 2, E-23071, Jaén, Spain (jmarti@ujaen.es.)